Proceedings of ERAD (2002): 190–194 © Copernicus GmbH 2002

ERAD 2002

Water vapor observations with SAR, microwave radiometer and GPS: comparison of scaling characteristics

D. N. Moisseev[1], **R. F. Hanssen**[2], **and F. J. van Leijen**[2]

[1]Physical, Geometrical and Space Geodesy, Faculty of Civil Engineering and Geosciences, Delft University of Technology, Thijsseweg 11, 2629JA Delft, The Netherlands
[2]Mathematical Geodesy and Positioning, Faculty of Civil Engineering and Geosciences, Delft University of Technology, Thijsseweg 11, 2629JA Delft, The Netherlands

Abstract. The knowledge of spatial distributions of water vapor is very important in atmospheric studies. Often satellite observations, for instance AVHRR, are used to study spatial distributions of water vapor. This method, however, has a limited spatial resolution of about 1 km and does not cover the entire atmospheric column. An alternative way to estimate the spatial behavior of the water vapor is to use temporal observations of the wet delay as given by GPS systems and water vapor paths as measured by microwave radiometers (MWR). These measurements can provide us, under certain conditions, with high-resolution spatial observations of water vapor. Recently, a new technique for atmospheric monitoring was proposed – based on differential satellite interferometric synthetic aperture radar (InSAR) delay measurements. This new method allows for high-resolution full column atmospheric mapping. In this article we focus on the comparison of scaling properties of water vapor as measured with SAR interferometry, GPS and microwave radiometer. We show that under current processing conditions the GPS time series do not provide a useful tool for studying scaling properties of water vapor. The MWR and InSAR, on the other hand, prove to be very useful instruments for this study.

1 Introduction

The knowledge of spatial distributions of water vapor is not only important in climate studies, weather forecasting but it is also important information for geodetic observations of the earth surface. Even though in the case of geodetic observations the atmosphere represents the unwanted component of a signal, given knowledge of the earth surface behavior, one can obtain very accurate information on the state of atmosphere at the time of measurements. A well-known example of this approach is the use of GPS for the retrieval of water vapor profiles (Bevis et al., 1992).

Correspondence to: D. N. Moisseev
(D.Moisseev@citg.tudelft.nl)

In this article we focus on the use of a relatively new geodetic technique, synthetic aperture radar interferometry (InSAR), for the investigation of scaling properties in the atmospheric water vapor distribution. SAR interferometry allows for the retrieval of 2D integrated water vapor distributions with a very high spatial resolution, in the order of 20 m, provided that the local typography is known and there are no surface deformations (Hanssen et al., 1999).

For this study a commonly used ground-based microwave radiometer and GPS provide us with temporal measurements of the integrated water vapor. Using wind measurements and assuming a "frozen" atmosphere (Taylor, 1938; Treuhaft, 1987) one can translate these temporal measurements into the spatial distribution of water vapor. Thus, spatial scaling properties as obtained from SAR can be compared to ones retrieved from the time-series measurements with GPS and microwave radiometer (MWR).

For the study presented in this paper the SAR measurements of ERS were used. The microwave radiometer data was obtained during the Clouds and Radiation (CLARA) campaign (van Lammeren et al., 2000) and GPS measurements are recorded by the Active GPS Reference System for the Netherlands (AGRS.NL).

In Sect. 2 of this paper GPS and MWR measurements of atmospheric water vapor are compared. It is shown that GPS measurements do not provide reliable information on atmospheric water vapor scaling behavior especially for studying short wavelength atmospheric phenomena. In Sect. 3 a short description of the SAR measurement technique is given. It is shown that InSAR measurements can provide a very precise estimate of differential integrated precipitable water vapor spatial distribution. Moreover, the water vapor measurements with MWR are used to validate the InSAR measurements. It is shown that theses two techniques provide comparable results. The InSAR measurements, even though providing the difference between two atmospheric states, can be more advantageous for some application since they provide high-resolution 2D water vapor maps as opposite to MWR, which only provides 1D profiles.

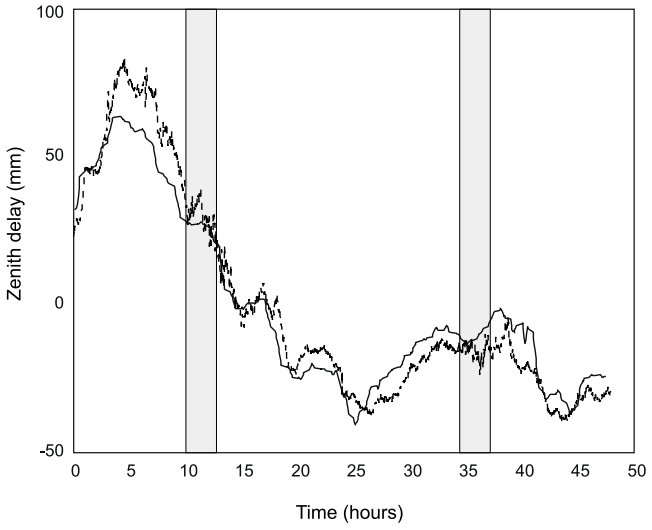

Fig. 1. Zenith wet delay measurements from 23 April 00:00 UTC to 24 April 23:51 UTC, carried out with GPS (solid line) and MWR (dashed line). The GPS and MWR measurements were taken during the CLARA campaign. The gray rectangle represents the 2.3 hours interval, centered around the SAR acquisitions, taken at 10:30 UTC.

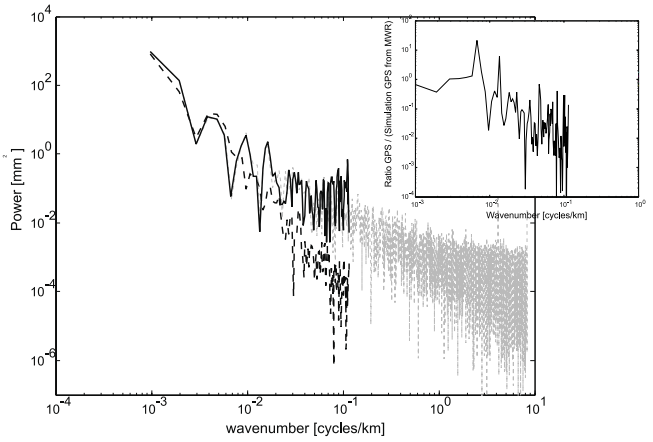

Fig. 2. Power spectra of GPS and MWR zenith wet delay measurements, taken on 23 April 1996. A scaling factor of 10 m/s was used to translate the temporal to spatial scales. The gray line represents the power spectrum of the MWR water vapor measurements; the sampling frequency is 1/5 Hz. The dashed line depicts the power spectrum of GPS observations; the measurements have the temporal resolution of 6 min. The solid line shows the power spectrum of the simulated GPS time series as calculated from MWR observations. The inserted figure shows the ratio of power spectra of the simulated GPS measurements to the true GPS power spectrum.

2 Comparisons of the water vapor measurements with GPS and microwave radiometer

During the CLARA cloud measurement campaign the 20/30/50 GHz microwave radiometer of Eindhoven University of Technology and the GPS receiver of Delft University of Technology (DUT) were collocated on the roof of the Department of Electrical Engineering, DUT. These two instruments allow one to retrieve the time series of integrated water vapor paths. In Fig. 1 the 48 hours time series, from 23 April 1996, 00:00 UTC to 24 April 1996, 23:51 UTC, of the zenith delay are shown. The MWR measurements are translated to the zenith delay, to facilitate comparisons with GPS and later with InSAR measurements. To reduce the influence of calibration of the brightness temperatures (Niell et al., 2001) to MWR and to compensate for the ionospheric and hydrostatic delays in the GPS measurements, the mean delays, calculated over the complete data series, were subtracted from these measurements. The time resolution of the MWR measurements is 5 sec and the observations of GPS were averaged over 6 min. In Fig. 1 one can see that these two observations are very similar, although the GPS measurements are lacking higher frequencies, as one would expect. In Fig. 2. power spectra of the GPS and MWR measurements are shown. For these calculations only data collected on 23 April 1996 was used. Furthermore, the temporal scales were translated to the spatial scales by applying a conversion factor of 10 m/s. It can be clearly seen that the spectra of GPS and MWR zenith wet delay measurements are different. To simulate the GPS like observation scheme, the MWR observations were averaged over 6 minutes, the resulting power spectrum shown in Fig. 2 as the thick solid line. Additionally, the ratios between the simulated and true GPS power spectra were calculated for measurements taken on 15–23 April, the averaged ratio is given in the insert in the Fig. 2. It can be seen that the simulated and the true power spectra of GPS delays are different and the ratio of these two spectra shows reduction of the power in the higher frequencies. Two steps in the processing of the GPS signals can explain this effect. Firstly, to translate GPS signals from different satellites to a zenith delay one should assume that there are no horizontal variations in the GPS delay measurements, and thus the zenith delay can be estimated by using a mapping function (Niell, 1996; Hanssen, 2001). Secondly, a Kalman filter is used to further smooth observations. As a result, the scaling properties of the zenith delays as obtained from GPS observations cannot be used for studying most of atmospheric phenomena, or they are at least of a less value than satellite observations.

3 InSAR atmospheric water vapor observations

The ERS-1 and ERS-2 SAR measurements provide a high resolution, 4×20 m, 2D measurements of the earth surface. A phase value of every resolution cell is defined as a superposition of the term which corresponds to the geometric distance, a term which correspond to propagation effects and the term which represents the scattering within the resolution cell (Hanssen, 2001). By creating an interferogram, effectively the phases corresponding to two measurements are subtracted from each other and if objects within resolution cells did not move and did not change from one acquisition to the other, the differential phase is mainly defined by the propagation effects and the difference in observation geome-

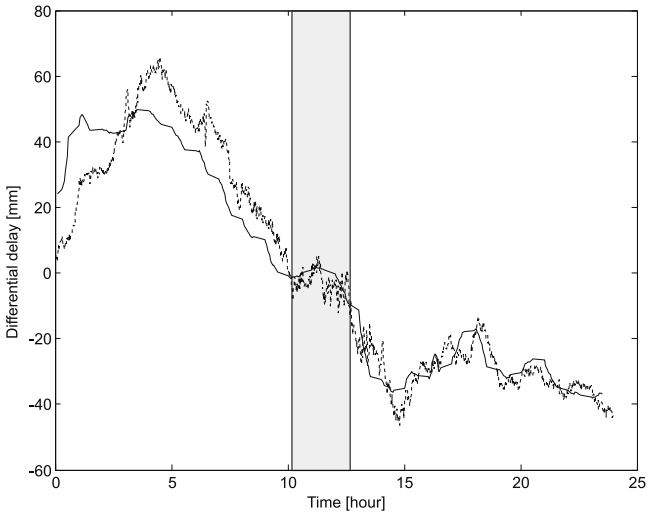

Fig. 3. Difference of zenith wet delay measurements at 23 and 24 April, carried out with GPS (solid line) and MWR (dashed line). The GPS and MWR measurements were taken during CLARA campaign on 23 and 24 April 1996. The gray rectangle represents the 2.3 hours interval, centered around the SAR acquisitions, taken at 10:30 UTC.

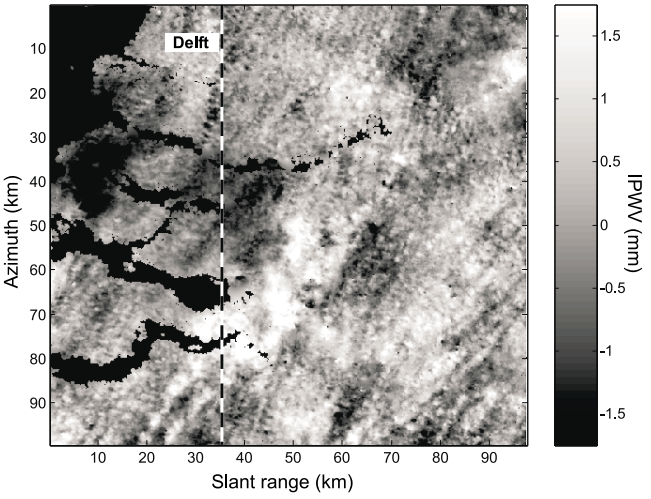

Fig. 4. Differential SAR interferogram of 23 and 24 April 1996, 10:38 UTC. The interferometric phase was translated to differential precipitable water vapor. The dashed line represents a best-fit profile based on MWR delay observations.

tries. Furthermore, if a reference elevation model is available one can remove the topographic phase component. After applying a simple cosine mapping function (Hanssen, 2001) and converting phases into the delays, the residual interferometric signal gives the differential zenith delays for the given pair of observations.

3.1 Observations

One interferogram using ERS-1 and ERS-2 SAR observations taken on 23 and 24 April 1996, was calculated and is shown in Fig. 4. Using a reference elevation model (TDN/MD, 1997) for the observation area a differential interferogram is obtained. Furthermore, the hydrostatic and ionospheric delay components were eliminated by subtracting the mean delay value, calculated over the complete image. The residual differential delays are mainly caused by difference in integrated precipitable water vapor from one observation to the other (Hanssen, 2001).

Also the time series of the differential zenith delays as measured by MWR were calculated by subtracting MWR observations taken on 23 and 24 April, see Fig. 3. Unfortunately only MWR observations on 24 April are only available at 60 sec resolution; therefore the observations from 23 April were down sampled to the same resolution.

3.2 Comparison of InSAR and MWR observations

For translation of temporal MWR measurements to the spatial observations, one needs to know the wind speed. Furthermore, for comparison between InSAR and MWR water vapor profiles information on the wind direction is required. Even though the wind information was available during our observations, there is a great variation in observed wind speeds and directions. On 23 April the radiosonde measurements showed strong winds of 10–15 m/s, from SSW. On 24 April the wind is weaker and is about 8–10 m/s, from WSW.

To improve the comparison of MWR measurements to InSAR observations, the MWR profile was rotated and stretched over the InSAR image (van der Hoeven et al., 2002). The wind speed and rotational angle that corresponded to the highest correlation between the two profiles were used to convert MWR time series to the spatial delay measurements. The resulting trace of the best-fit profile is shown by dashed line on Fig. 4 and the resulting InSAR and MWR profiles are given in Fig. 5. It was found that the best conversion factor is 14 m/s, which is roughly corresponding to the wind speed on 23 April. Moreover, the best-fit wind direction is also more close to the wind direction during 23 April. This result can be easily explained, since the delay signal range was larger on 23 April, as can be seen in Fig. 1, and thus delay signal from this day dominates the differential delay.

In Fig. 5 we can see that delay profiles as measured with MWR and InSAR are showing the same trends and only differ in some higher frequency details. It should be noted that the correlation between these two measurements is found to be 0.68. For further comparisons of the MWR and InSAR water vapor measurements, the power spectra of the profiles are calculated. The resulting spectra are shown in Fig. 6, it should be noted that the available MWR measurements only have temporal resolution of 60 sec and thus only the part of the spectrum located at the frequencies lower than 10^{-1} (cycles/km) can be trusted. In this part of the spectrum there is a good agreement between observed scaling properties of MWR and InSAR measurements. Moreover, the MWR mea-

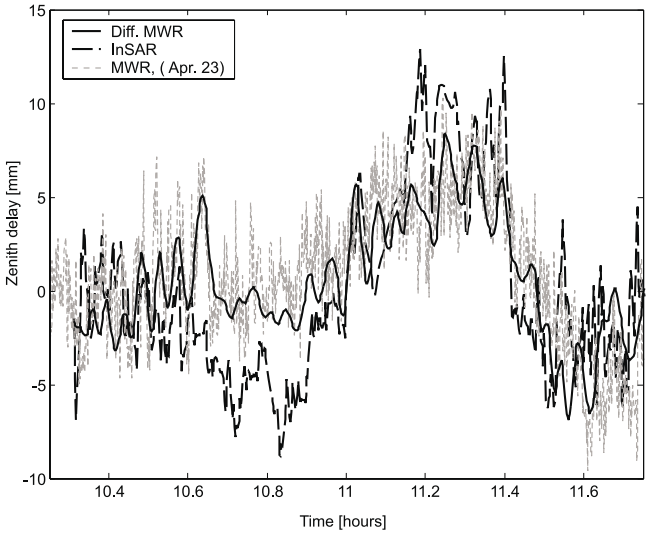

Fig. 5. The differential zenith delay profiles, as observed by MWR and InSAR. The InSAR profile represents the best fit of the MWR time series through the interferogram. The fit was calculated by changing the scaling factor from 1 to 20 m/s, changing the mean wind direction from 0 to 180 degrees and by time coregistering the observations. The resulting scaling factor is 14 m/s and the correlation between these two profiles is 0.68. Also a MWR time serie of measurements that were taken on 23 April is plotted as thick gray dashed line. These measurements were taken with the 5 s time sampling.

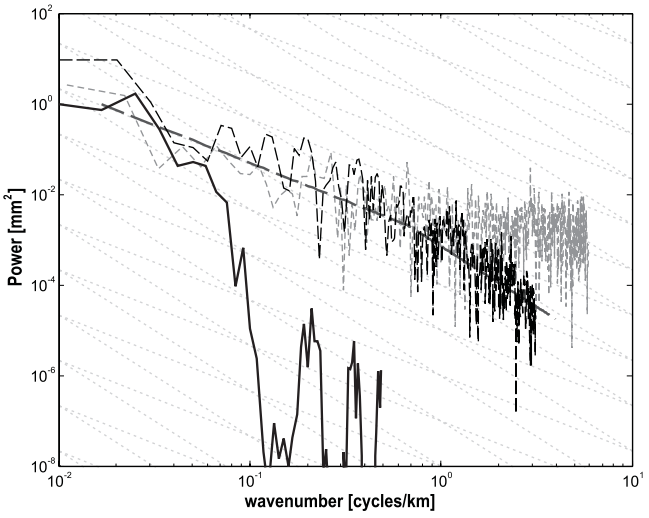

Fig. 6. The power spectra of the MWR time series (solid line) and the best fit InSAR profile (the dashed thin line). The dashed thick line represents the modeled scaling behavior of the wet delay as observed by InSAR, the model was initiated by the MWR observations at the scale 1/50 (cycles/km). The thin dotted lines represent 8/3 and 5/3 power laws. It should be noted that the temporal resolution of the MWR measurements in this case is 60 sec, and as a result there is a strong reduction of the signal for wavenumbers larger than 10^{-1} cycles/km. Also the power spectrum of MWR measurements that were taken on 23 April are plotted as gray thick dashed line. This measurement has time resolution of 5 s.

surements at this scales can be used to initiate a turbulence model as described by Hanssen (2001) to characterize properties of the atmospheric water vapor at the other scales. The thick dashed line in Fig. 6 gives the result of this modeling.

4 Conclusions and recommendations

In this paper the scaling properties of atmospheric water vapor were studied using GPS, MWR and InSAR. It was shown that GPS measurements are not suitable for studies of atmospheric phenomena, where variations at the smaller wavelengths play an important role. On the example of one inteferogram, taken during CLARA campaign, and the MWR observations we have shown that the radiometer and the SAR measurements show comparable results, provided that the full-resolution radiometer data is available. The InSAR measurements, however, can be more advantageous for some application since they provide high-resolution 2D water vapor maps as opposite to MWR, which only provides 1D profiles. The main drawback of InSAR measurements, however, is that only relative atmospheric measurements are currently possible. Nonetheless, this drawback can be overcome if larger number of interferograms of the same area is available.

Acknowledgement. The authors would like to thank the ESA for providing the ERS-1, 2 SAR measurements. The microwave radiometer measurements were kindly provided by CLARA participants.

References

Bevis, M., Businger, S., Herring, T. A., Rocken, C., Anthes, R. A., and Ware, R. H., 1992. GPS meteorology: Remote sensing of atmospheric water vapor using the Global Positioning System. Journal of Geophysical Research 97: 15,787-15,801.

Hanssen, R. F., 2001. Radar Interferometry. Data interpretation and error analysis. Kluwer Academic Publishers, Dordrecht, The Netherlands.

Hanssen, R. F., Weckwerth, T. M., Zebker, H. A. and Klees, R., 1999. High- resolution water vapor mapping from interferometric radar measurements. Science 283, 1295-1297.

Niell, A. E., 1996. Global mapping functions for the atmosphere delay at radio wavelengths. Journal of Geophysical Research 101, 3227-3246.

Niell, A. E., Coster, A. J., Solheim, F. S., Mendes, V. B., Toor, P. C., Langley, R. B., and Upham C. A., 2001. Comparison of measurements of atmospheric wet delay by radiosonde, water vapor radiometer, GPS, and VLBI. Journal of Atmospheric and Oceanic Technology 18, 830-850.

Taylor, G.I., 1938. The spectrum of turbulence. Proceedings of the Royal Society London, Series A CLXIV, 476-490.

TDN/MD, 1997. Top Hoogte MD digital elevation model. Topografische Dienst Nederland and Meetkundige Dienst Rijkswaterstaat.

Treuhaft, R.N. and Lanyi, G. E., 1987. The effect of the dynamic wet troposphere on radio interferometric measurements. Radio Science 22, 251-265.

van der Hoeven, A., Hanssen, R. F. and Ambrosius, B., 2002. Tropospheric delay estimations and analysis using GPS and SAR

interferometry. Physics and Chemistry of the Earth 27, 385-390.
van Lammeren, A., Feijt, A. V., Donovan, D., Bloemink, H., Russchenberg, H., Venema, V., Erkelens, J., Apituley, A., Brink, H. T., Khlystov, A., Jongen, S., Brussaard, G. and Herben, M., 2000. CLARA: Clouds and radiation- intensive measurement campaigns in the Netherlands. In: Proc. Of Symposium on Remote Sensing of Clouds Parameters: Retrieval and Validation, Delft, The Netherlands, pp. 5-10.